Flux-driven turbulence simulation of L-H transition with BOUT++ code

Haruki SETO and Masatoshi YAGI
Japan Atomic Energy Agency, Aomori, Japan

collaborating with

Xueqiao. Xu[a]
[a]Lawrence Livermore National Laboratory, CA, USA

OUTLINE

- Motivation for L-H transition simulation by BOUT++
- L-H transition model by flux-driven RMHD model
- Preliminary results by 2-field L-H transition model
- Summary and Future Works

Motivation for L-H transition simulation by BOUT++ (1/2)

L-H transition simulation activity in JAEA [M. Yagi CPP2012]

- L-H transition by integrated transport simulation framework
  - TOPICS (1.5D core transport)
  - SONIC (2D SOL transport)
  - CDBM turbulent model
- Spontaneous turbulence quench and pedestal formation
- CDBM turbulent model has free parameters controlling
  - L-H transition power threshold
  - HH-factor

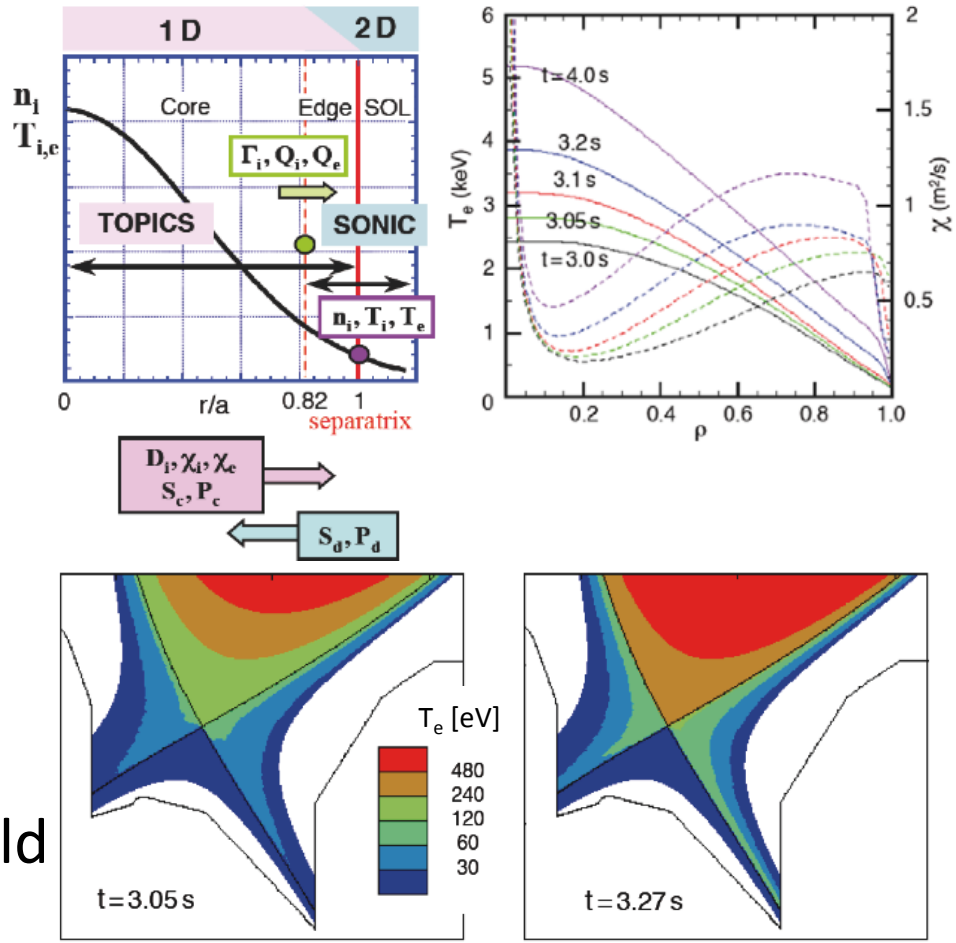

For more self-consistent simulation of L-H transition, CDBM turbulent transport model should be improved

Motivation for L-H transition simulation by BOUT++ (2/2)

CDBM turbulent transport model is based on

- Current Diffusive Ballooning Mode (CDBM) turbulence
- Turbulence suppression by mean flow shear

CDBM turbulent transport model can be improved by introducing missing physics

- Turbulence suppression by zonal flow shear
- SOL physics (geometry, impurities, neutrals)

BOUT++ framework can handle

- CDBM turbulence (resistive ballooning mode + hyper-resistivity)
- Mean flow shear
- Zonal flow shear
- Complex geometry including open filed (SND,DND,…)

Our goal is to reproduce L/H transition with CDBM turbulence by BOUT++ to get physical insights for improving CDBM turbulence model

OUTLINE

- Motivation for L-H transition simulation by BOUT++
- L-H transition model by flux-driven RMHD model
- Preliminary results by 2-field L-H transition model
- Summary and Future Works

L-H transition simulation by flux-driven 2-field RMHD

[slab: L. Chônè PoP2014, NF2015, torus: G.Y. Park PoP2015 (BOUT++)]

$$\partial_t \nabla_\perp^2 \phi + \{\phi, \nabla_\perp^2 \phi\} = -\nabla_\parallel^2 \phi - \mathrm{G}p + \boxed{\partial_x F_{neo}} + \nu_\perp \nabla_\perp^4 \phi$$

$$\partial_t p + \{\phi, p\} = \delta_c \mathrm{G}\phi + \chi_\parallel \nabla_\parallel^2 p + \chi_\perp \nabla_\perp^2 p + \boxed{S}$$

$$F_{neo} = -\mu_{neo}(\bar{p})[\partial_x \bar{\phi} - K_{neo}(\bar{p})\partial_x \bar{p}],$$ [L. Chônè PoP2014]

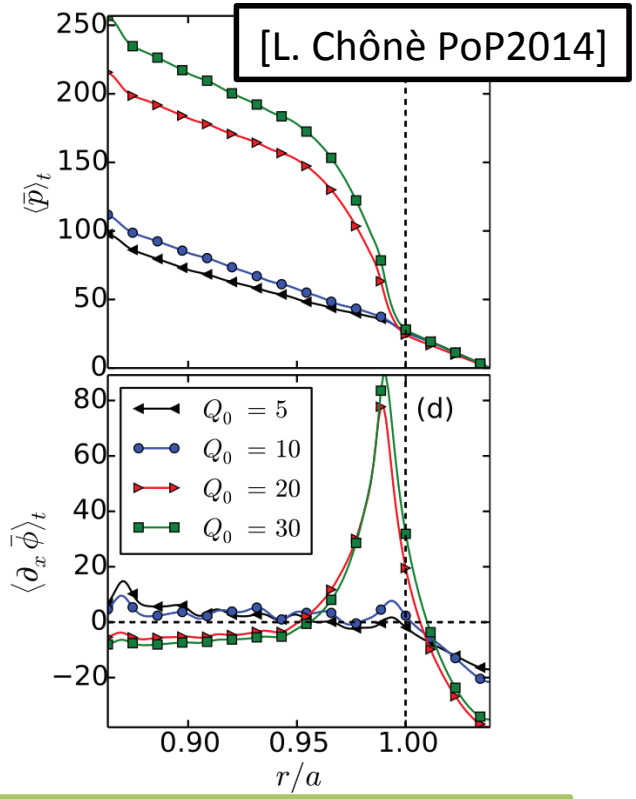

- RBM turbulence described by 2-field RMHD model
- Strongly sheared E_r driven by radial force balance with poloidal flow introduced as poloidal damping in vorticity equation
- Dynamic pressure profile determined by balance among turbulence transport, heat source and sink

If inflow heat flux Q_0 exceeds a threshold, strongly sheared E_r is generated and then turbulence transport level is suppressed in the edge region.

➡ Pedestal structure is formed in accordance with a new dynamic heat balance

Physical background of poloidal damping term (1/2)

Poloidal damping term is derived from parallel viscous force

- Heuristic closure of parallel viscous force [T.A. Gianakon PoP2002]

$$\nabla \cdot \overleftrightarrow{\Pi}_{\|\mathrm{i}} = m_\mathrm{i} n_\mathrm{i} \frac{\langle B^2 \rangle}{B_\theta^2} \left(\mu_{\mathrm{i}1} \bar{V}_{\mathrm{i}\theta} + \mu_{\mathrm{i}2} \frac{2\bar{q}_{\mathrm{i}\theta}}{5\bar{p}_\mathrm{i}} \right) \boldsymbol{e}_\theta, \quad \boldsymbol{e}_\theta = \sqrt{g} \nabla\zeta \times \nabla\psi, \quad \boldsymbol{B} = \nabla\zeta \times \nabla\psi + B_\zeta \nabla\zeta$$

- Mean poloidal rotation by radial force balance ($n_\mathrm{i} = \mathrm{const.}, \bar{V}_{\mathrm{i}\perp} \gg \bar{V}_{\mathrm{i}\|}$)

$$\nabla \bar{P}_\mathrm{i} \cdot \nabla\psi = e_\mathrm{i} n_\mathrm{i} \left(\bar{\boldsymbol{E}} + \bar{\boldsymbol{V}}_\mathrm{i} \times \boldsymbol{B} \right) \cdot \nabla\psi \rightarrow \bar{V}_{\mathrm{i}\theta} = \frac{\sqrt{g} |\nabla\psi|^2}{B_\zeta} \left[\frac{d}{d\psi} \left(\bar{\phi} + \frac{P_\mathrm{i}}{e_\mathrm{i} n_\mathrm{i}} \right) + \cancel{\bar{V}_\mathrm{i}^\zeta} \right]$$

- Mean poloidal heat flow by parallel neoclassical force balance

$$\frac{2\bar{q}_{\mathrm{i}\theta}}{5\bar{p}_\mathrm{i}} = -\frac{\mu_{\mathrm{i}1}}{\mu_{\mathrm{i}2}} V_{\mathrm{i}\theta}^{\mathrm{nc}}, \quad V_{\mathrm{i}\theta}^{\mathrm{nc}} = \frac{\sqrt{g} |\nabla\psi|^2}{B_\zeta} k_\mathrm{i} \frac{d}{d\psi} \left(\frac{\bar{P}_\mathrm{i}}{e_\mathrm{i} n_\mathrm{i}} \right) \qquad k_\mathrm{i} = -\frac{\mu_{\mathrm{i}2}}{\mu_{\mathrm{i}1}}$$

Parallel viscous force results in friction force expressing radial force balance with neoclassical poloidal flow ($\langle B^2 \rangle \sim B_t^2 \sim B_0^2 \gg B_p^2$)

$$\nabla \cdot \overleftrightarrow{\Pi}_{\|\mathrm{i}} = m_\mathrm{i} n_\mathrm{i} \frac{\langle B^2 \rangle}{B_\theta^2} \mu_{\mathrm{i}1} \left(\bar{V}_{\mathrm{i}\theta} - \bar{V}_{\mathrm{i}\theta}^{\mathrm{nc}} \right) \boldsymbol{e}_\theta \simeq m_\mathrm{i} n_\mathrm{i} \mu_{\mathrm{i}1} \frac{B_0^2}{B_p^2} \left[\frac{\boldsymbol{B}_0 \times \nabla\bar{\phi}}{B_0^2} + (1 - k_\mathrm{i}) \frac{\boldsymbol{B}_0 \times \nabla\bar{P}_\mathrm{i}}{e_\mathrm{i} n_\mathrm{i} B_0^2} \right]$$

Physical background of poloidal damping term (2/2)

- Poloidal damping term in torus geometry

$$\boldsymbol{b}_0 \cdot \nabla \times \left(\nabla \cdot \overleftrightarrow{\Pi}_{\mathrm{i}\parallel}\right) = m_{\mathrm{i}} n_{\mathrm{i}} \mu_{\mathrm{nc}} \left[\nabla_\perp^2 \frac{\bar{\phi}}{B_0} - k_{\mathrm{nc}} \nabla_\perp^2 \frac{\bar{P}_{\mathrm{i}}}{e_{\mathrm{i}} n_{\mathrm{i}} B_0} - \nabla_\perp k_{\mathrm{nc}} \cdot \nabla_\perp \frac{\bar{P}_{\mathrm{i}}}{e_{\mathrm{i}} n_{\mathrm{i}} B_0}\right]$$

$$+ m_{\mathrm{i}} n_{\mathrm{i}} \nabla_\perp \mu_{\mathrm{nc}} \cdot \left[\nabla_\perp \frac{\bar{\phi}}{B_0} - k_{\mathrm{nc}} \nabla_\perp \frac{\bar{P}_{\mathrm{i}}}{e_{\mathrm{i}} n_{\mathrm{i}} B_0}\right], \quad \mu_{\mathrm{nc}} = \mu_{\mathrm{i}1} \frac{B_0^2}{B_p^2}, \quad k_{\mathrm{nc}} = k_{\mathrm{i}} - 1$$

  - First term in RHS is consistent with $\partial_x F_{neo}$ in slab limit
  - This expression is consistent with G.Y. Park's damping term

- Interpolation formulae for neoclassical flow coefficients
  - Neoclassical parallel viscosity [Callen IAEA 1986]

$$\mu_{\mathrm{i}1} = \frac{0.66\epsilon^{1/2}\nu_{*\mathrm{i}}}{(1 + 1.03\nu_{*\mathrm{i}}^{1/2} + 0.31\nu_{*\mathrm{i}})(1 + 0.66\nu_{*\mathrm{i}}\epsilon^{3/2})}$$

  - Neoclassical friction coefficient [Hinton & Hazeltine RMP1976]

$$k_{\mathrm{i}} = \frac{1}{1 + \nu_{*\mathrm{i}}^2 \varepsilon^3}\left(\frac{1.17 - 0.35\nu_{*\mathrm{i}}^{1/2}}{1 + 0.7\nu_{*\mathrm{i}}^{1/2}} - 2.1\nu_{*\mathrm{i}}^2\varepsilon^3\right)$$

They are functions of collisionality and vary largely across collisionality regimes → Strongly sheared E_r is generated in the edge region

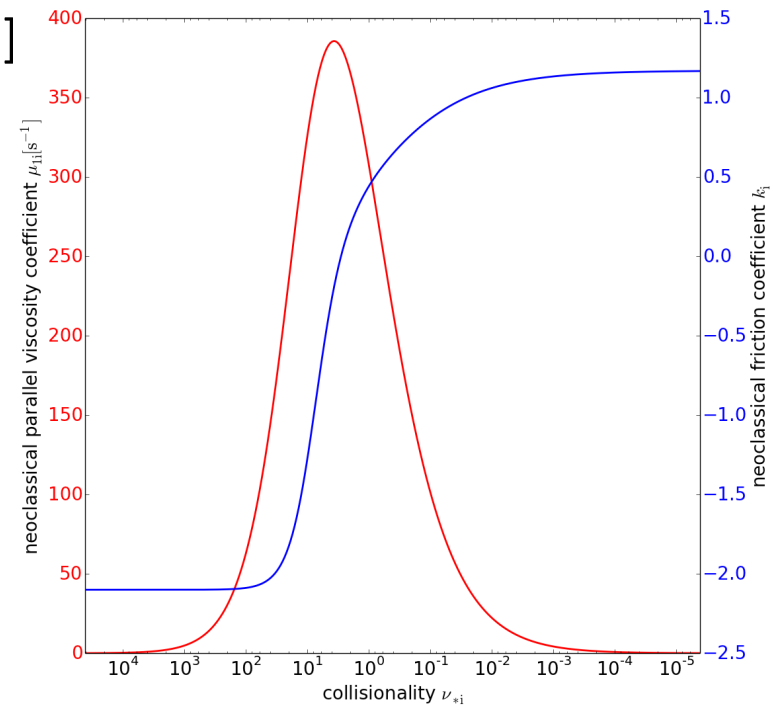

L-H transition model with CDBM turbulence

We have been developing a BOUT++ physics module for L-H transition with CDBM turbulence from elm-pb module

$$
\begin{aligned}
\frac{\partial U}{\partial t} =& -[\phi, U] - \frac{1}{2}\left(-[\phi, U] + \left[F, \nabla_\perp^2 \phi\right] + \nabla_\perp^2 [\phi, F]\right) \\
& - \left[\mu_{\mathrm{nc}}\left(\nabla_\perp^2 \bar{\phi} - \delta_{\mathrm{i}} k_{\mathrm{nc}} \nabla_\perp^2 \bar{p} - \delta_{\mathrm{i}} \nabla_\perp k_{\mathrm{nc}} \cdot \nabla_\perp \bar{p}\right) + \nabla_\perp \mu_{\mathrm{nc}} \cdot \left(\nabla_\perp \bar{\phi} - \delta_{\mathrm{i}} k_{\mathrm{nc}} \nabla_\perp \bar{p}\right)\right] \\
& - B_0^2 \nabla_\parallel J + \boldsymbol{b}_0 \times \boldsymbol{\kappa} \cdot \nabla_\perp p + \mu_\perp \nabla_\perp^2 U + \mu_\parallel \nabla_\parallel^2 U \\
\frac{\partial Y}{\partial t} =& -[\phi, Y] - \frac{1}{B_0} \partial_\parallel (B_0 \phi) + \delta_{\mathrm{i}} \nabla_\parallel p + \eta J - \lambda \nabla_\perp^2 J \\
\frac{\partial p}{\partial t} =& -[\phi, p] - \beta_* \left[2 \boldsymbol{b}_0 \times \boldsymbol{\kappa} \cdot \nabla_\perp \phi + 2 \delta_{\mathrm{i}} B_0^2 \nabla_\parallel J\right] + \chi_\perp \nabla_\perp^2 p + \chi_\parallel \nabla_\parallel^2 p + S_p - \bar{p} L_p
\end{aligned}
$$

$$
\begin{aligned}
U =& \nabla_\perp^2 F, \quad F = \phi + \delta_{\mathrm{i}} p, \quad J = \nabla_\perp^2 \psi, \quad Y = \psi - d_{\mathrm{e}}^2 J \\
\beta_* =& \frac{\gamma p}{1 + \gamma p / 2 B_0^2}, \quad d_a = \frac{c}{R_0} \sqrt{\frac{\epsilon_0 m_a}{n_a e_a^2}}, \quad \delta_a = \frac{d_a}{4 B_0}, \quad [f, g] = \boldsymbol{b}_0 \cdot \nabla_\perp f \times \nabla_\perp g, \\
\partial_\parallel =& \boldsymbol{b}_0 \cdot \nabla, \quad \nabla_\parallel = \boldsymbol{b}_0 \cdot \nabla - [\psi,], \quad \nabla_\perp = \nabla - \nabla_\parallel, \quad \nabla_\perp^2 = \nabla^2 - \nabla_\parallel^2
\end{aligned}
$$

OUTLINE

- Motivation for L-H transition simulation by BOUT++
- L-H transition model by flux-driven RMHD model
- Preliminary results by 2-field L-H transition model
- Summary and Future Works

Simulation setup

- ES-RBM model w/o 2-fluid effects

$$\frac{\partial U}{\partial t} = -[\phi, U] - B_0^2 \nabla_\parallel J + \boldsymbol{b}_0 \times \boldsymbol{\kappa} \cdot \nabla_\perp p + \mu_\perp \nabla_\perp^2 U$$
$$- \mu_{\rm nc} \left[\nabla_\perp^2 \bar{\phi} - \delta_{\rm i} k_{\rm i}^{\rm nc} \nabla_\perp^2 \bar{p} - \delta_{\rm i} \nabla_\perp k_{\rm i}^{\rm nc} \cdot \nabla_\perp \bar{p}\right]$$
$$\frac{\partial p}{\partial t} = -[\phi, p] + \chi_\perp \nabla_\perp^2 p + \chi_\parallel \nabla_\parallel^2 p + \alpha_S(t) S - \bar{p} L$$
$$U = \nabla_\perp^2 \phi, \quad J = \frac{1}{\eta B_0} \partial_\parallel (B_0 \phi)$$
$$\eta = 1.0 \times 10^{-5}, \quad \mu_\perp = \chi_\perp = 1.0 \times 10^{-6}$$
$$\chi_\parallel = 1.0 \times 10^{-1}, \quad n_0 = 1.0 \times 10^{19} [\mathrm{m}^{-3}]$$

- Circular equilibrium w/o shift

$$q(\rho) = 1.0 + 2.0(\rho/0.95)^3, \quad q = 3 \text{ at } \rho = 0.95$$
$$a_0 = 0.5[\mathrm{m}], \quad R_0 = 2.0[\mathrm{m}], \quad \bar{B} = 2.0[\mathrm{T}]$$

Source amplitude is set to lower level until turbulence is driven ($t<7000t_A$).
Source amplitude is ramped up to double ($7000t_A < t < 9000t_A$) and is kept constant at higher level ($9000t_A < t < 15000t_A$).

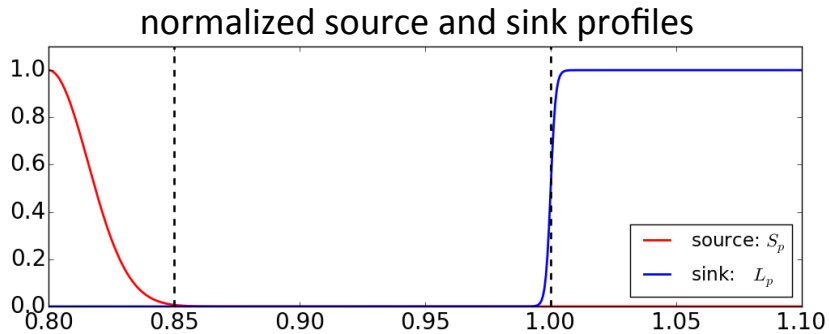

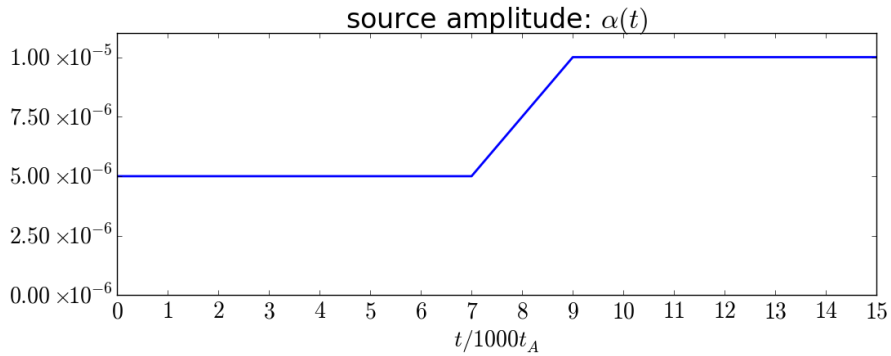

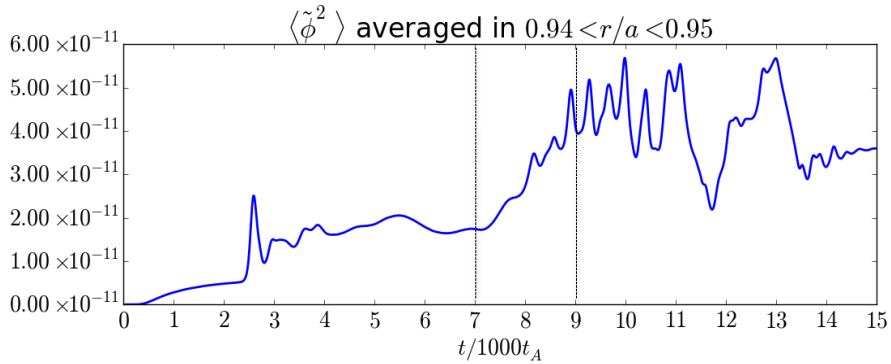

Spatiotemporal structure of turbulence intensity

- During source intensity ramp-up ($7000t_A$~$9000t_A$), turbulence grows up at q=3 and has oscillating structure ($9000t_A$~$11000t_A$)
- Turbulence is suppressed to lower level and its radial structure is also localized in narrow domain when strongly sheared E_r exits in the edge region ($11000t_A$~$15000t_A$) (next slide)

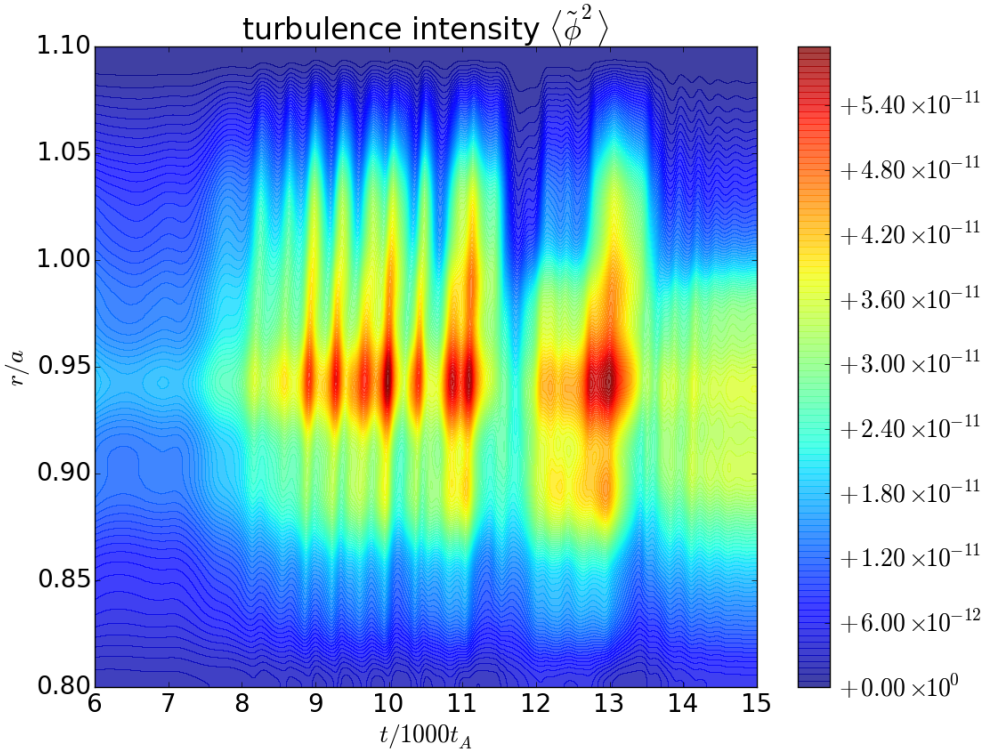

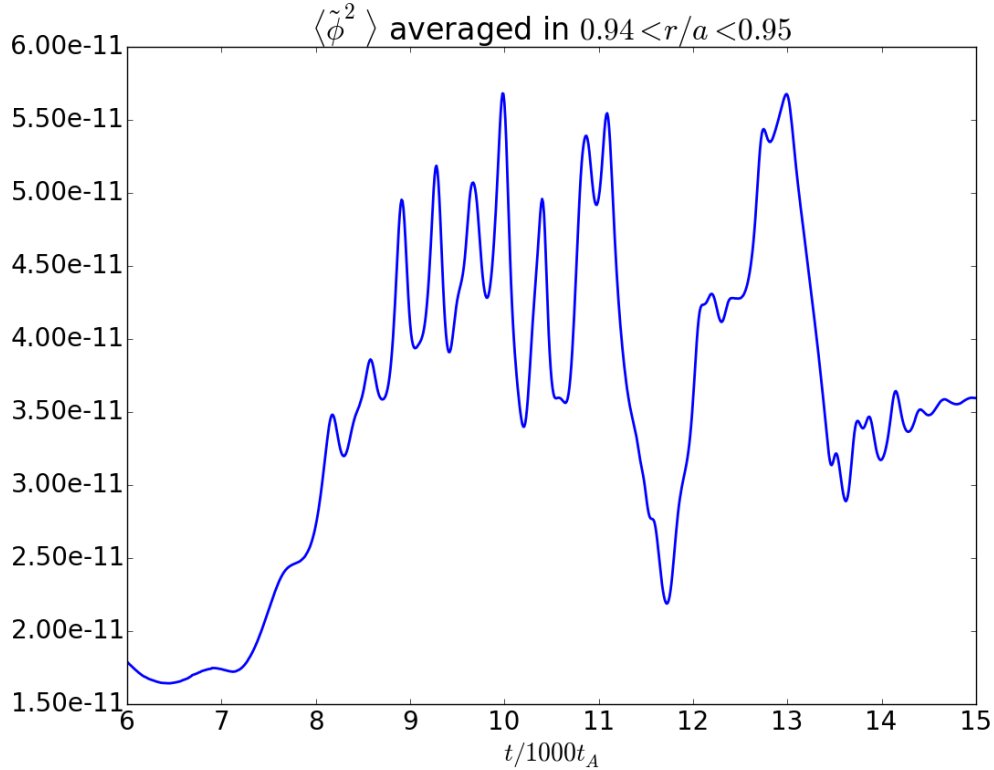

Spatiotemporal structure of mean radial electric field

- After source intensity ramp-up, radial electric field at the edge region oscillates with similar amplitudes and then changes drastically
- Radial electric field is strongly sheared at the edge region when turbulence is suppressed

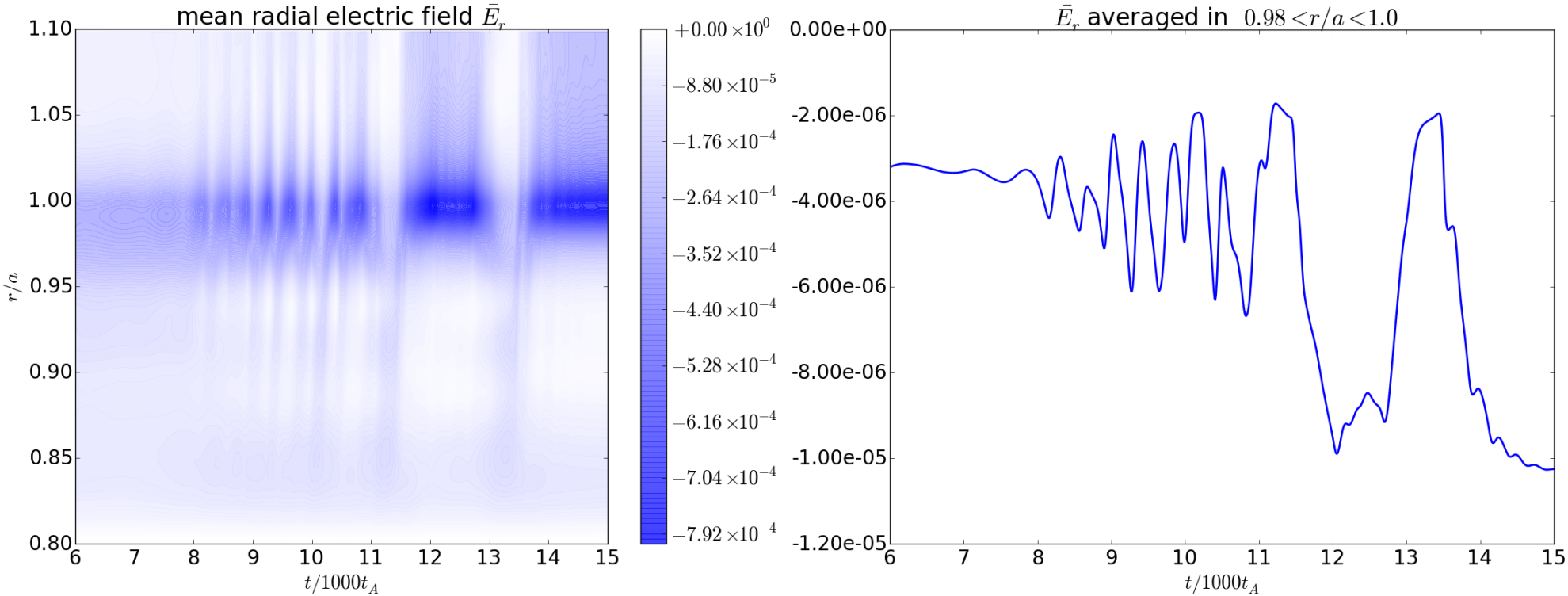

Spatiotemporal structure of mean pressure

- Pressure gradient front expands to the outer region when turbulence is suppressed to lower level and shrinks to inner region when turbulence is excited to higher level.

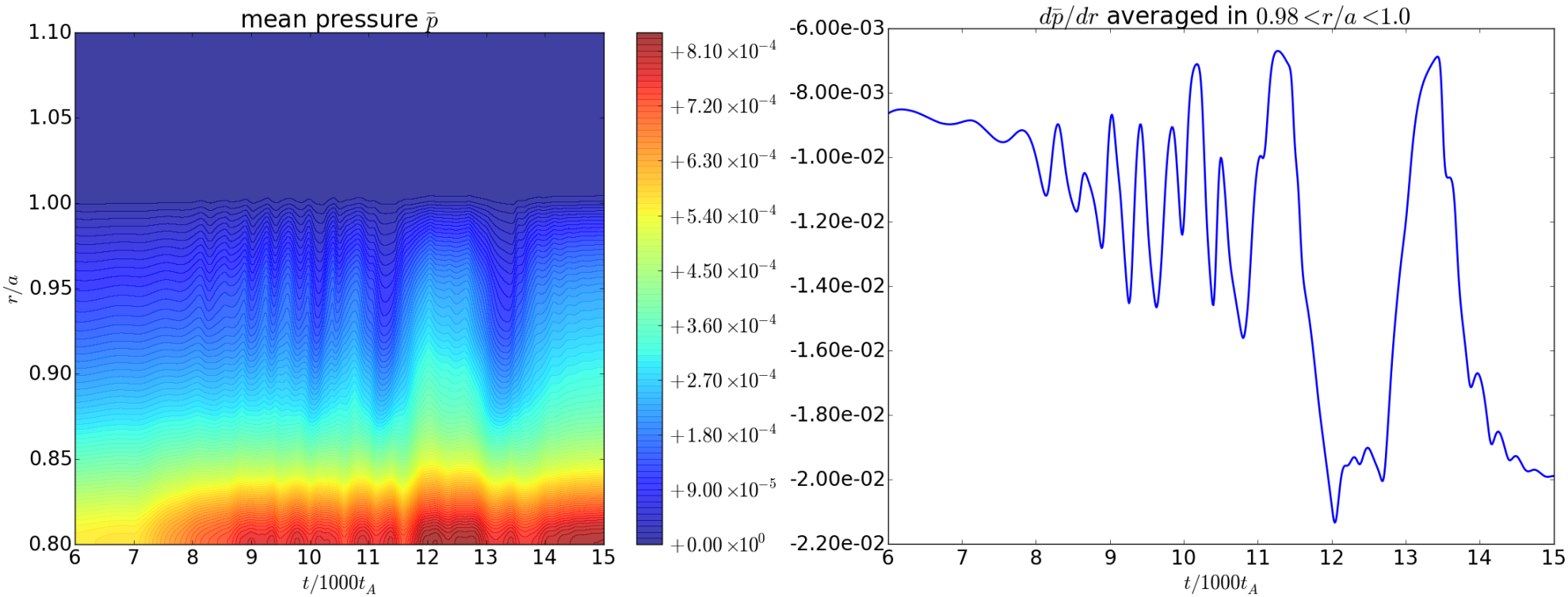

Temporal evolution of toroidal mode spectrum ϕ_n averaged in 0.94 < r/a < 0.95

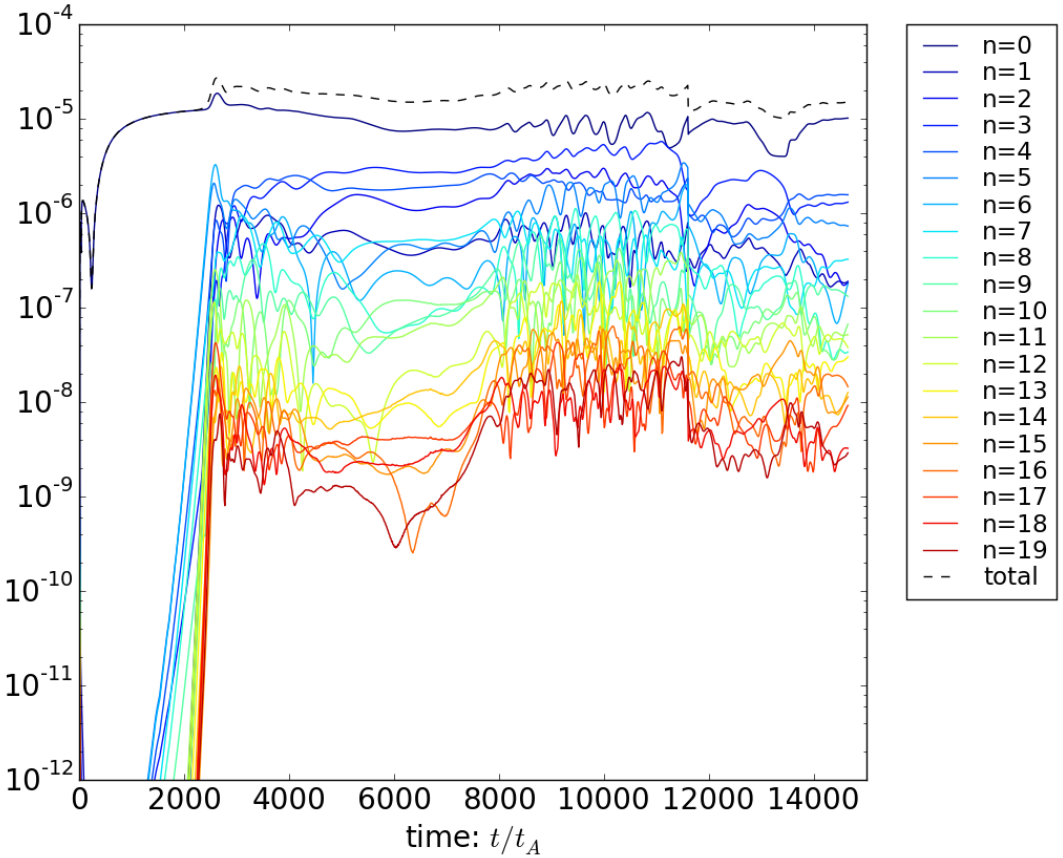

- n < 10 modes are dominant modes in our simulation
- If our module solves ES-RBM turbulence correctly, dominant modes should be n =10~20
- Inflow energy to (0,0)-mode may leak to low-n modes through unphysical channels (numerical nonlinearity in 3rd WENO?)

OUTLINE

- Motivation for L-H transition simulation by BOUT++
- L-H transition model by flux-driven RMHD model
- Preliminary results by 2-field L-H transition model
- Summary and Future Works

Summary and Future work

Summary

- Some key features related to L-H transition by flux-driven RMHD model are observed
  1. steeply sheared E_r at the edge by poloidal damping effect
  2. turbulence suppression at the edge by mean flow shear
  3. energy deposition at the edge by dynamic energy balance

Future work

- Identification of root causes of energy leak problem
- parameter scan for L-H transition

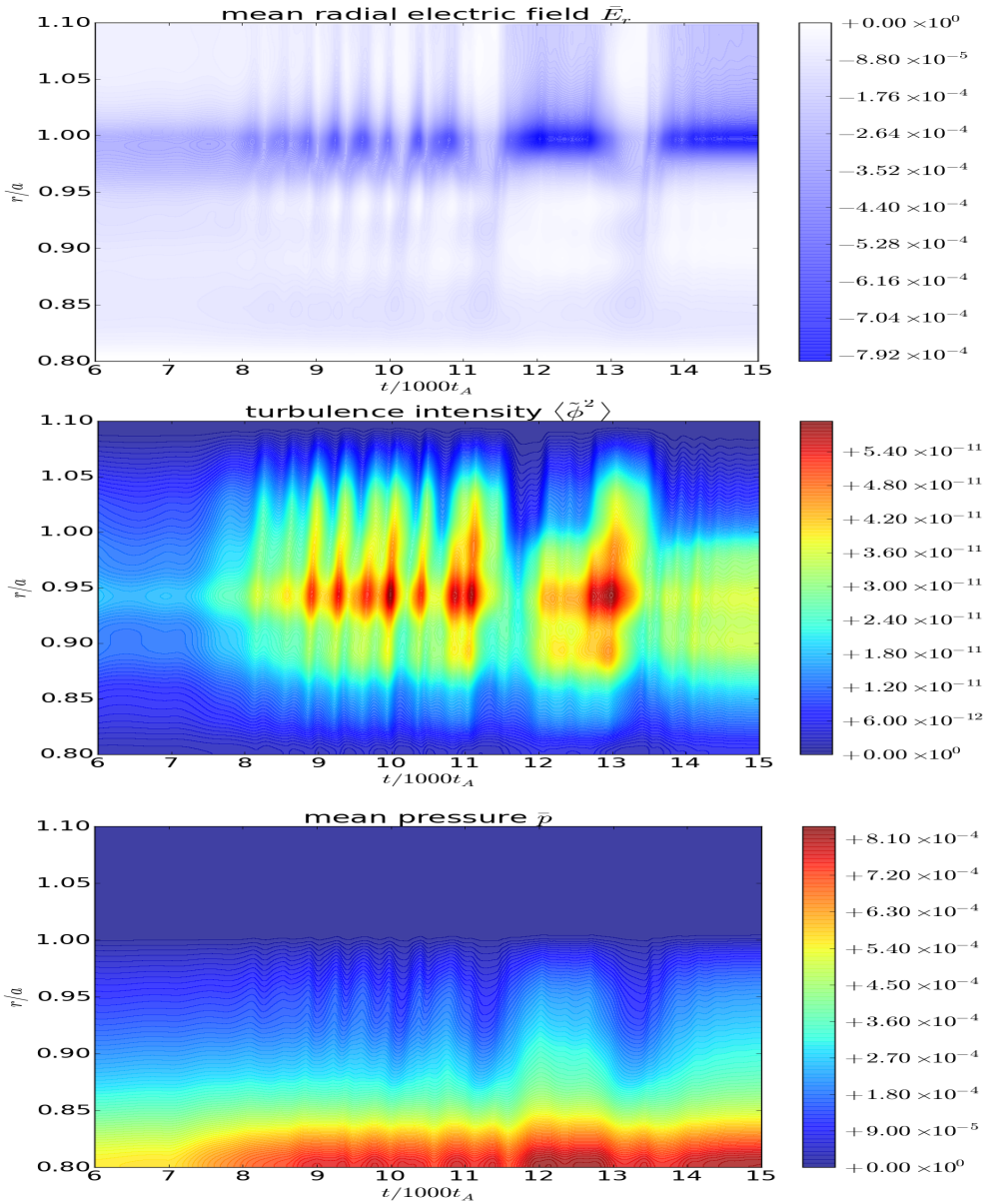

Back Slides

Sensitivity of neoclassical coefficients to ion temperature


```
# input parameters
R0   = 2.0          # major radius [m]
a0   = 0.5          # minor radius [m]
n0   = 1.e19        # number density [m-3]
B0   = 2.0          # magnetic intensity [T]
Ai   = 2.0          # ion mass in mp unit
lnA  = 20.0         # Coulomb logarithm
Zi   = 1.0          # Z effective
q    = 3.0          # safty factor at rho = 1
```

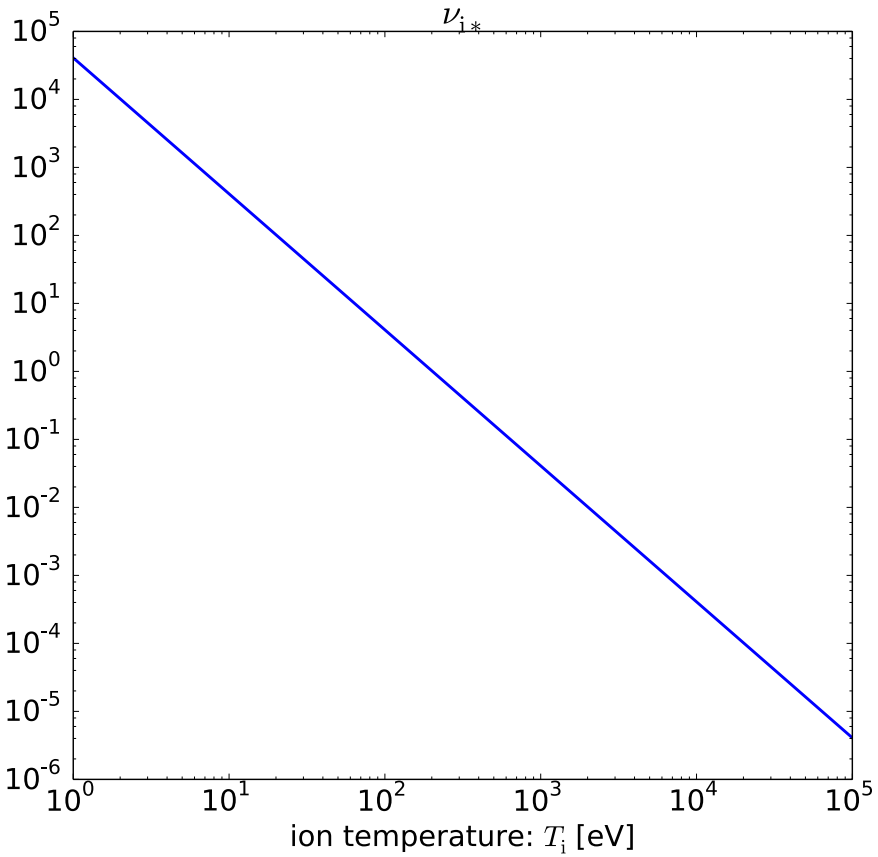

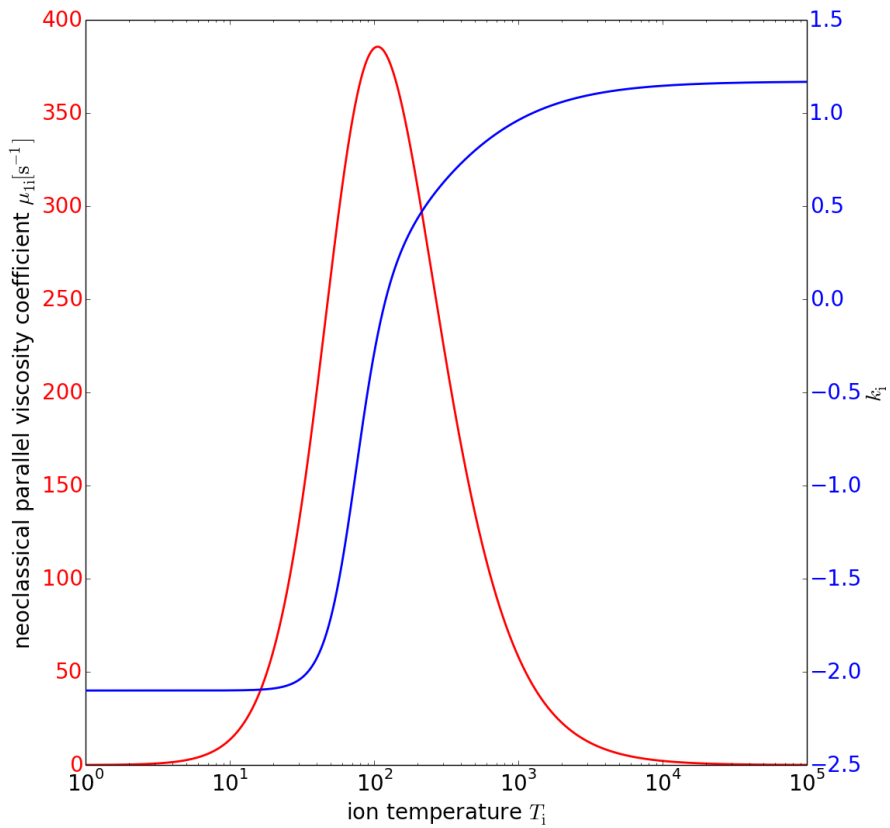

Spatiotemporal structure of mean ion temperature

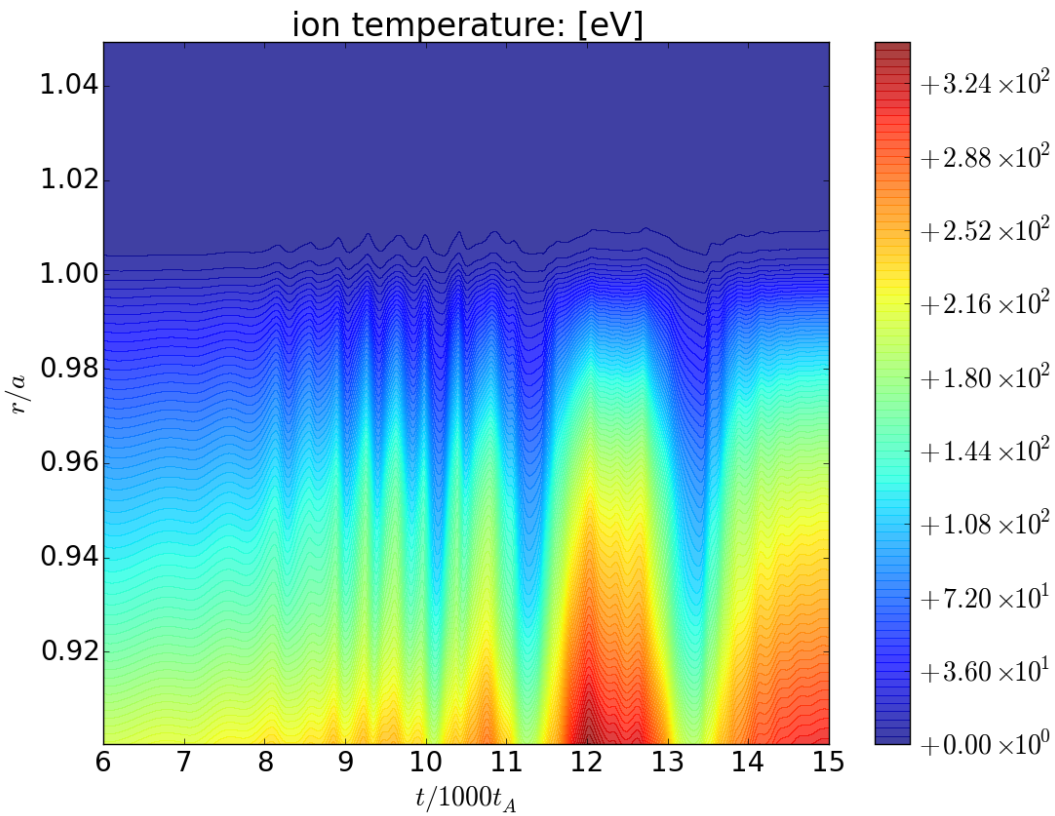

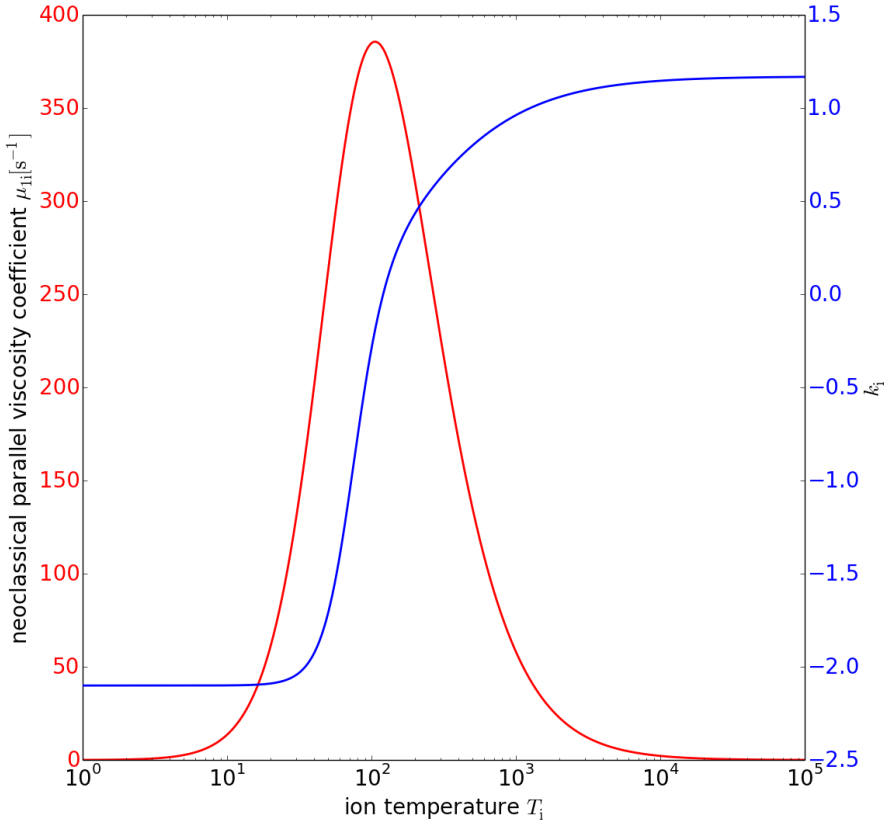

Unphysical mode transition in linear multi-n RBM simulation: setup (1/2)

- **Linear 3-field RBM**

$$\frac{\partial U_1}{\partial t} = -B_0^2 \nabla_{\parallel} J_1 + \boldsymbol{b}_0 \times \boldsymbol{\kappa} \cdot \nabla P_1$$
$$\frac{\partial P_1}{\partial t} = -\boldsymbol{b}_0 \cdot \nabla \phi_1 \times \nabla P_{\mathrm{eq}}$$
$$\frac{\partial \psi_1}{\partial t} = -\frac{1}{B_0} \nabla_{\parallel} \left(B_0 \phi_1 \right) + \eta J_1$$
$$U_1 = \nabla_{\perp}^2 \phi_1, \;\; J_1 = \nabla_{\perp}^2 \psi_1, \;\; \nabla_{\parallel} = \boldsymbol{b}_0 \cdot \nabla$$

- **Circular equilibrium w/o shift**

$$q(\rho) = 1.0 + 2.0 \left(\frac{\rho}{0.75} \right)^2$$
$$P_{\mathrm{eq}}(\rho) = \frac{\beta_{\mathrm{p}}}{2} \left\{ 1.0 + \tanh \left[10(\rho - 0.75) \right] \right\}$$
$$\beta_{\mathrm{p}} = 0.01, \quad \eta = 1.0 \times 10^{-6}$$
$$a_0 = 0.5[\mathrm{m}], \quad R_0 = 2[\mathrm{m}], \quad \bar{B} = 2[\mathrm{T}]$$

Simulation results in this slides were calculated by rmhd-lh.cxx not by elm-pb.cxx

- **Computational domain**

$$x = \psi - \psi_0, \quad y = \theta, \quad z = \zeta - \int_{\theta_0}^{\theta} \nu(\psi, \theta) d\theta$$
$$0.5 \le \rho(x) \le 1.0, \quad 0 \le y \le 2\pi, \quad 0 \le z \le 2\pi/5$$
$$Nx \times Ny \times Nz = 516 \times 128 \times 65$$

- **Boundary conditions and toroidal filtering settings**
  - bndry_all = dirichlet on U_1, P_1, ϕ_1 , J_1
  - bndry_xin and _xout = zerolaplace on ψ_1
  - Inversion flags on ϕ_1 are dirichlet on both x boundaries
  - low_pass_z = 8 (n=0,5,…,40)

Two BOUT.inp employing same parameters except parameters of differencing scheme are used in this slide (next slide)

Unphysical mode transition in linear multi-n RBM simulation: setup (2/2)

- w/Upwind-case (default)
  - advection terms declared by b0xGrad_dot_Grad are calculated by 3rd order WENO
  - advection terms declared by bracket are also calculated by 3rd order WENO

```
##################################################
# derivative methods

[ddx]

first  = C4 # order of first x derivatives (options are 2 or 4)
second = C4 # order of second x derivatives (2 or 4)
upwind = W3 # order of upwinding method (1, 4, 0 = TVD (DO NOT USE), 3 = WENO)

[ddy]

first  = C4
second = C4
upwind = W3

[ddz]

first  = C4  # Z derivatives can be done using FFT
second = C4
upwind = W3

#######################################################
# BRACKET_METHOD flags:
# 0:BRACKET_STD; derivative methods will be determined
#   by the choices C or W in this input file
# 1:BRACKET_SIMPLE; 2:BRACKET_ARAKAWA; 3:BRACKET_CTU.

bm_exb_flag = 0
bm_mag_flag = 0
```

- w/o Upwind-case
  - advection terms declared by b0xGrad_dot_Grad are calculated by 4rd order central differencing
  - advection terms declared by bracket are calculated by ARAKAWA scheme

```
##################################################
# derivative methods

[ddx]

first  = C4 # order of first x derivatives (options are 2 or 4)
second = C4 # order of second x derivatives (2 or 4)
upwind = C4 # order of upwinding method (1, 4, 0 = TVD (DO NOT USE), 3 = WENO)

[ddy]

first  = C4
second = C4
upwind = C4

[ddz]

first  = C4  # Z derivatives can be done using FFT
second = C4
upwind = C4


#######################################################
# BRACKET_METHOD flags:
# 0:BRACKET_STD; derivative methods will be determined
#   by the choices C or W in this input file
# 1:BRACKET_SIMPLE; 2:BRACKET_ARAKAWA; 3:BRACKET_CTU.

bm_exb_flag = 2
bm_mag_flag = 2
```

Growth rates of ϕ in w/ and w/o upwind-case

- Unphysical mode jumps occur in w/ Upwind-case but those don't occur in w/o Upwind-case
- Unphysical mode jump may be driven by nonlinear up-winding scheme (System is linearized theoretically but has nonlinearity numerically)
- In w/o Upwind-case numerical oscillation of n=0 mode grows but it may be stabilized by dissipation term

w/ Upwind-case (default)

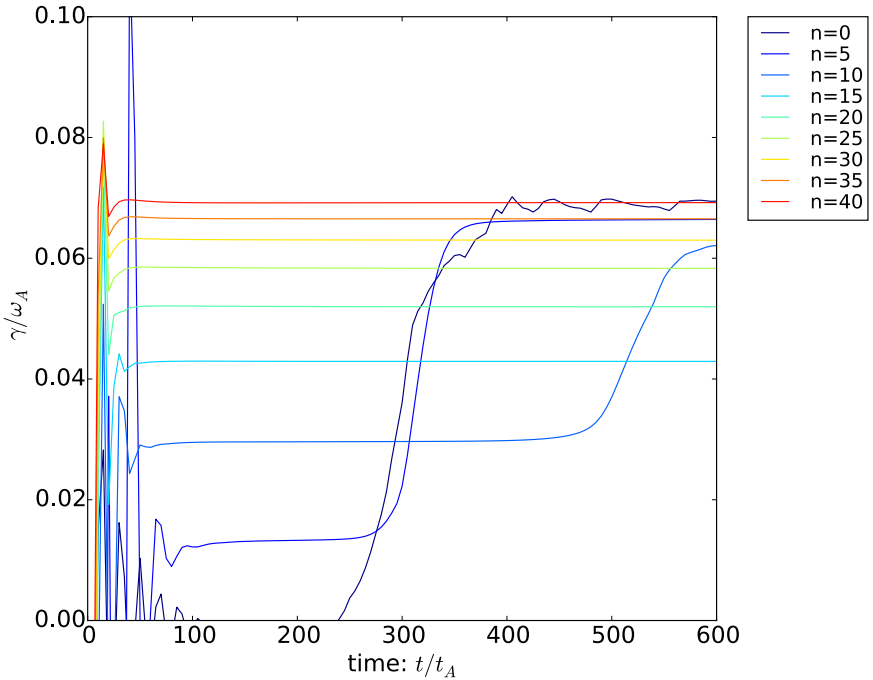

w/o Upwind-case

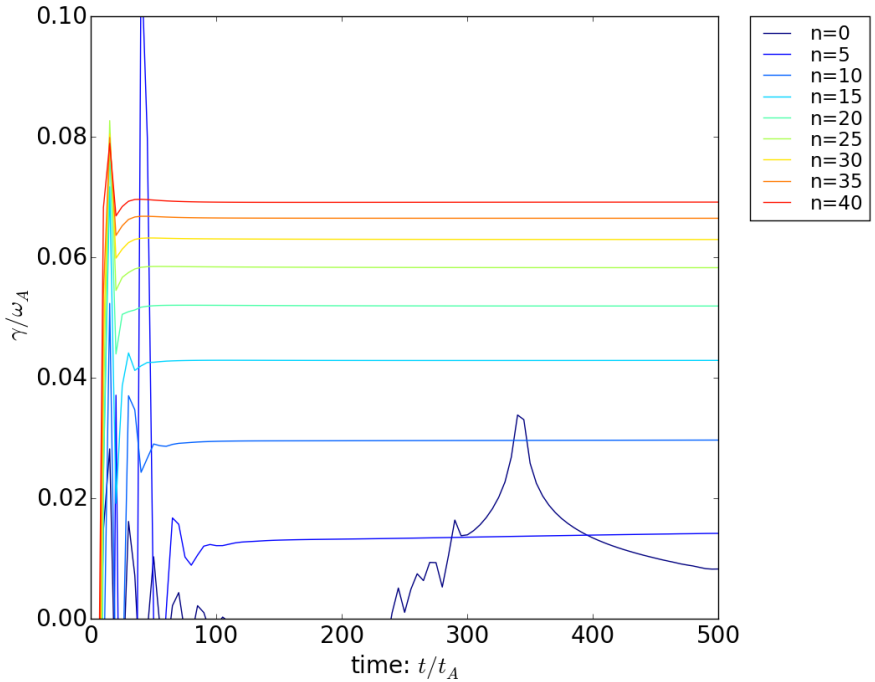

Temporal evolution of ϕ in w/ and w/o upwind-case

w/ Upwind-case (default)

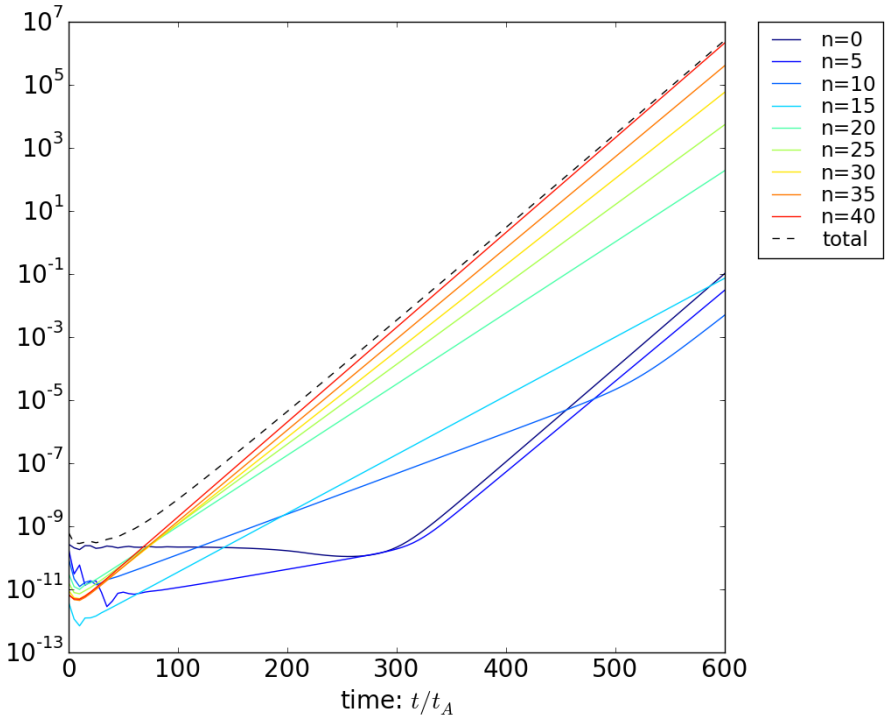

w/o Upwind-case

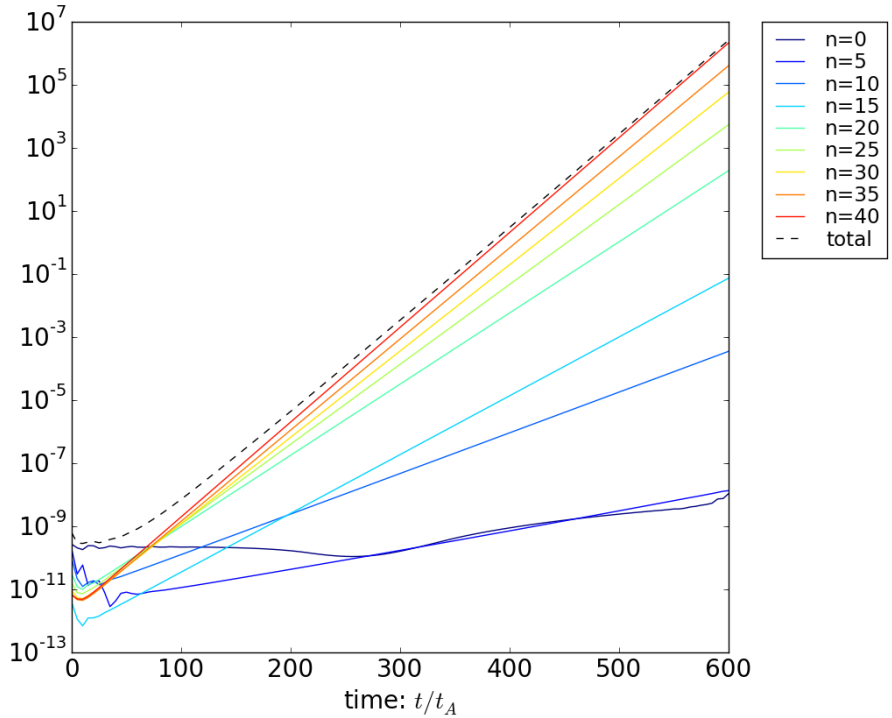

Poloidal slice of ϕ before and after mode transition in w/ and w/o upwind-case

- w/ Upwind n=10 before transition (t=300t_A)

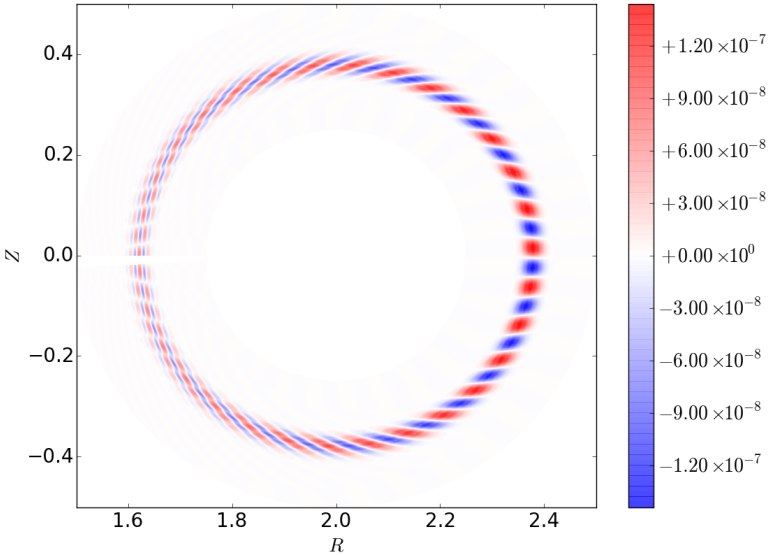

- w/o Upwind n=10 before transition (t=300t_A)

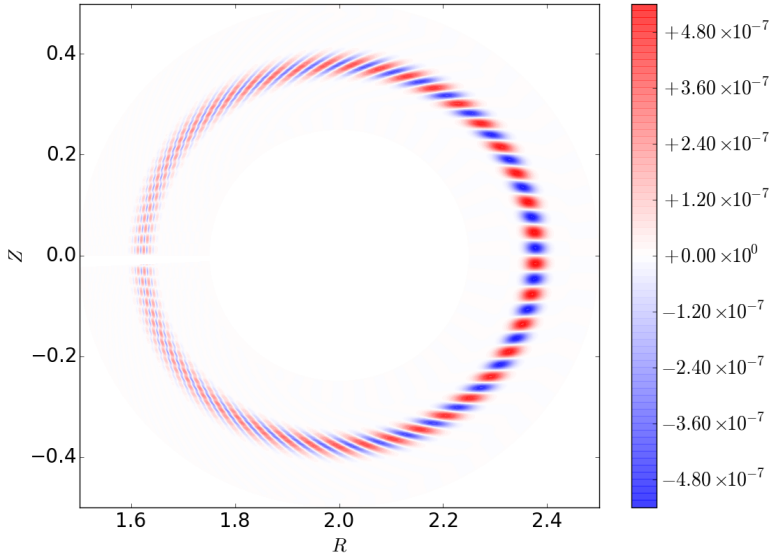

- w/ Upwind n=10 after transition (t=600t_A)

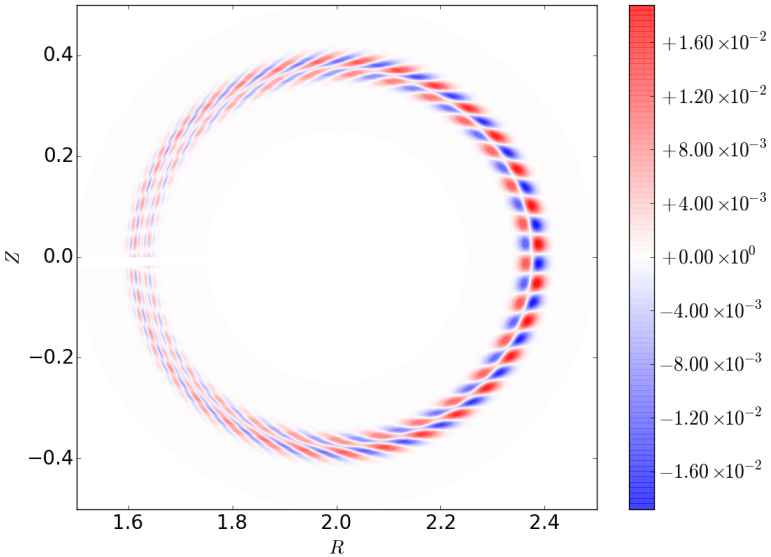

- w/o Upwind n=10 after transition (t=600t_A)

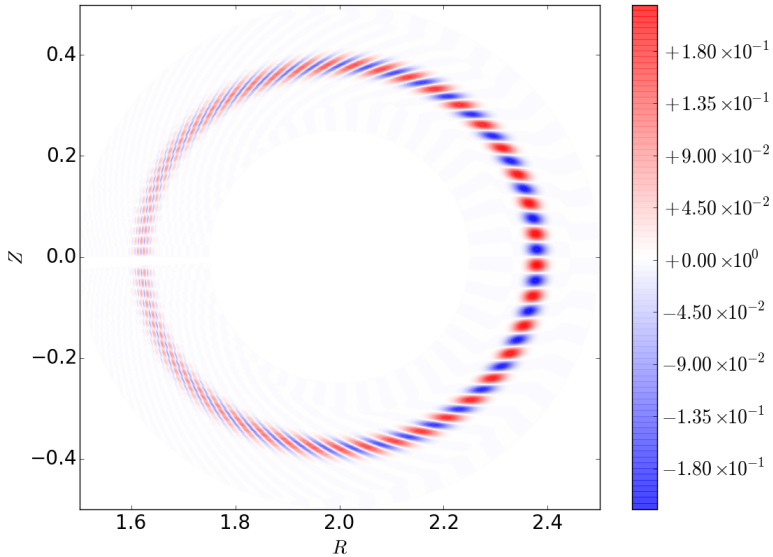

Implementation of 3rd WENO in BOUT++

BOUT/src/sys/derivs.cxx

```
/// 3rd-order WENO scheme
BoutReal VDDX_WENO3(stencil &v, stencil &f) {
  BoutReal deriv, w, r;

  if(v.c > 0.0) {
    // Left-biased stencil

    r = (WENO_SMALL + SQ(f.c - 2.0*f.m + f.mm)) / (WENO_SMALL + SQ(f.p - 2.0*f.c + f.m));
    w = 1.0 / (1.0 + 2.0*r*r);

    deriv = 0.5*(f.p - f.m) - 0.5*w*(-f.mm + 3.*f.m - 3.*f.c + f.p);

  }else {
    // Right-biased

    r = (WENO_SMALL + SQ(f.pp - 2.0*f.p + f.c)) / (WENO_SMALL + SQ(f.p - 2.0*f.c + f.m));
    w = 1.0 / (1.0 + 2.0*r*r);

    deriv = 0.5*(f.p - f.m) - 0.5*w*( -f.m + 3.*f.c - 3.*f.p + f.pp );
  }

  return v.c*deriv;
}

/// 3rd-order CWENO. Uses the upwinding code and split flux
BoutReal DDX_CWENO3(stencil &f) {
  BoutReal a, ma = fabs(f.c);
  // Split flux
  a = fabs(f.m); if(a > ma) ma = a;
  a = fabs(f.p); if(a > ma) ma = a;
  a = fabs(f.mm); if(a > ma) ma = a;
  a = fabs(f.pp); if(a > ma) ma = a;

  stencil sp, vp, sm, vm;

  vp.c = 0.5; vm.c = -0.5;

  sp = f + ma;
  sm = ma - f;

  return VDDX_WENO3(vp, sp) + VDDX_WENO3(vm, sm);
}
```